Taylor & Francis
Taylor & Francis Group

Journal of Maps

ISSN: (Print) (Online) Journal homepage: https://www.tandfonline.com/loi/tjom20

# Geomorphology of the Clarion Clipperton Zone, tropical North Pacific Ocean

John Parianos & Pedro Madureira

**To cite this article:** John Parianos & Pedro Madureira (2021) Geomorphology of the Clarion Clipperton Zone, tropical North Pacific Ocean, Journal of Maps, 17:2, 901-909, DOI: 10.1080/17445647.2021.2001387

**To link to this article:** https://doi.org/10.1080/17445647.2021.2001387

JOURNAL OF MAPS
2021, VOL. 17, NO. 2, 901–909
https://doi.org/10.1080/17445647.2021.2001387

SCIENCE

OPEN ACCESS Check for updates

# Geomorphology of the Clarion Clipperton Zone, tropical North Pacific Ocean

John Parianos[a] and Pedro Madureira[b,c]

[a]Cook Islands Seabed Minerals Authority, Avarua, Cook Islands; [b]Task Group for the Extension of the Continental Shelf (EMEPC), Paço de Arcos, Portugal; [c]Department of Geosciences and Institute of Earth Sciences, Évora University, Évora, Portugal

**ABSTRACT**

The Clarion Clipperton Zone (CCZ) hosts a valuable deposit of polymetallic nodules. Understanding the geology of this deposit is key to its effective exploration and future mining. Interpretation of satellite derived bathymetry elucidates large scale geomorphological units and structural units that characterize the area. The Main Map is includes distinct plains, rises, and lows of abyssal hills, steps and a trough along parts of the bounding fracture zone, seamount chains, fault zones and rifts.

**ARTICLE HISTORY**
Received 30 April 2021
Revised 25 October 2021
Accepted 25 October 2021

**KEYWORDS**
GEBCO bathymetry; multibeam bathymetry; Seabed geomorphology; Pacific Ocean; Polymetallic nodules

## 1. Introduction

The release of an updated global bathymetric product by GEBCO (British Oceanographic Data Centre, 2020) provides an opportunity to interpret the regional and local seabed bathymetry of the Clarion-Clipperton Zone (CCZ) oceanic plate segment at a large scale (1:6,000,000). The CCZ segment is a 6000 × 1000 km region in the tropical North Pacific (Figure 1). It contains polymetallic nodules, which accumulate manganese, nickel, copper and cobalt to levels that have reasonable prospects for eventual economic extraction (Menard & Shipek, 1958). In combination with other data, interpretation of the global bathymetric product (GEBCO grid) elucidates the geomorphological structure within the CCZ and, the systematics of this structure helps explain the formational history of the plate segment.

The interpreted age of the seafloor over the extent of the CCZ increases from east to west (Figure 1), consistent with increasing distance from the East Pacific Rise spreading centre (EPR). The seafloor deepens progressively from about ~4200 m at 115°W to ~4800 m at 128°W, then it varies between ~4800 m and ~5500 m until 161°W (Figure 1). The CCZ has other plate segments to its south (Clipperton – Galapagos segment) and north (Molokai – Clipperton segment), and there is a general increase in depth from south to north between the three segments (Figure 1). To the west the CCZ is bound by the Line Islands rise; further west is the Central Pacific Basin and the SE corner of the Pacific Triangle (Boschman & van Hinsbergen, 2016). To the east the CCZ is bound by the Mathematician Seamounts, further east is the EPR and the Rivera and northernmost Cocos microplates (Manea et al., 2013).

Polymetallic (also called ferro-manganese) nodules are found in all of the world's oceanic basins (McKelvey et al., 1983). The high Ni, Co, Cu, Mn grades in CCZ nodules are thought to result from: significant metal supply via net biological carbonate-silicate export from the surface; metal release near the nodules at the seabed via a combination of water depth relative to the lysocline; and distance from continental land masses resulting in an absence of competitor detrital sediments (International Seabed Authority, 2010a; Lipton et al., 2016; Morgan, 2003). High grade nodules are found at the seabed surface in a very soft clay – ooze – seawater mix termed as the semi-liquid layer or geochemically active layer (Bender et al., 1966; Callender & Bowser, 1980). These metals are adsorbed into the open structures of the slowly precipitating phyllomanganate minerals within the nodules. The 4500 km by 500 km extent of the CCZ nodule deposit can be approximated from exploration contracts issued by, as well as reserved areas held by, the International Seabed Authority (ISA) (International Seabed Authority, 2020), Figures 1 and 2.

No prior regional scale geomorphological maps of the CCZ are known. (Neizvestnov et al., 2004) and (Kotlinski et al., 2009) published a lineament and feature map and (Kazmin, 2003) and (International Seabed Authority, 2010b) reference some of the bathymetric rises and other features in the map (e.g. Eastern Central and Cooper Rises). CCZ scale maps of nodule chemistry, abundance, seabed sediment type are contained in (International Seabed Authority, 2010a) and

CONTACT John Parianos johnparianos@gmail.com

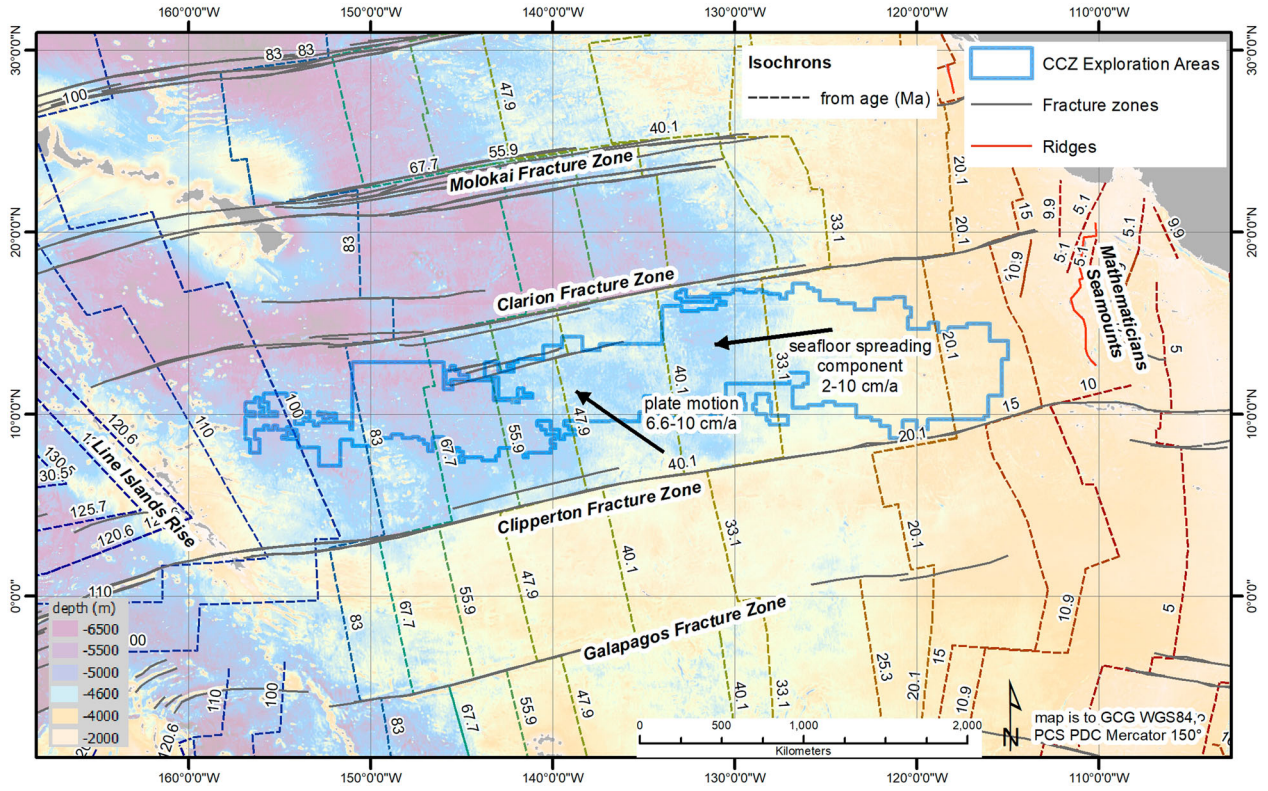


**Figure 1.** CCZ depths, basement ages and exploration areas of interest. Isochrons from (Müller et al., 2016), Fracture zones and ridges from (Matthews et al., 2011; Wessel et al., 2015), seafloor spreading & plate motion directions from (Morgan, 2003). Spreading rate from isochrons (last 100 Ma), plate motion back-track estimate from (Heiko Pälike et al., 2009) (accelerating over last 50 Ma).

(International Seabed Authority, 2010b). The interpretation described here is compatible with the higher-level global seabed classification of (Harris et al., 2014), and the habitat classification of (McQuaid et al., 2019).

The seabed in the CCZ is mostly composed of basaltic abyssal hills. These are typically covered in a variety of siliceous and calcareous sediment, e.g. (van Andel et al., 1975; Pälike et al., 2009). In much of the CCZ, thin and often poorly consolidated siliceous clays and oozes (Neogene to modern Clipperton Oceanic Formation) overly thicker calcareous nannofossil chalk (Eocene to Neogene Marquesas Oceanic Formation), that formed when the crust was located further south in the equatorial region (International Seabed Authority, 2010b). A third, mostly siliceous sedimentary unit is also found in the western part of the CCZ (Line Island Oceanic Formation).

The majority of abyssal hills are interpreted to have formed via normal faulting (i.e. horst and graben structures) in turn resulting from shrinking and subsiding driven by progressive plate cooling after formation at a spreading centre (Macdonald et al., 1996). Abyssal hills are not apparent in most of the GEBCO grid and can only be seen in 12 kHz multibeam coverage and along some ship-tracks. The hills are typically: around 100–300 m high (trough to crest); have a frequency of 1–5 km; and strike for ten to several hundred kilometres. In the central and eastern CCZ the abyssal hills mostly strike 350° (perpendicular to the direction of current plate spreading), while in the western CCZ the hills strike mostly N-S (Figure 3). Interspersed hills with an overall secondary strike are found in some areas, most commonly to ±010° (i.e. roughly perpendicular to the direction of plate motion).

A range of other morphological features are present and mostly only resolvable in the 12 kHz bathymetry and/or backscatter. These include:

- volcanic knolls from ~50 m in height, up to seamounts that rise ~4 kilometres above the surrounding seabed;
- outcropping dyke/fissure lavas and sheet flows that are interpreted to have formed in relatively recent times (i.e. post much of the sediment record); and
- potholes in the Marquesas Formation carbonate strata, see also (Fouquet & Depauw, 2014; Mayer, 1981; Moore et al., 2007). Note that seabed carbonates over much of the CCZ are currently unstable at this water depth relative to the interpreted position of the lysocline (Broecker, 2003; Chen et al., 1988).

## 2. Methods

The new interpretation in the map (also Figure 4) is based on the following data sources (e.g. Figures 3 and 4):

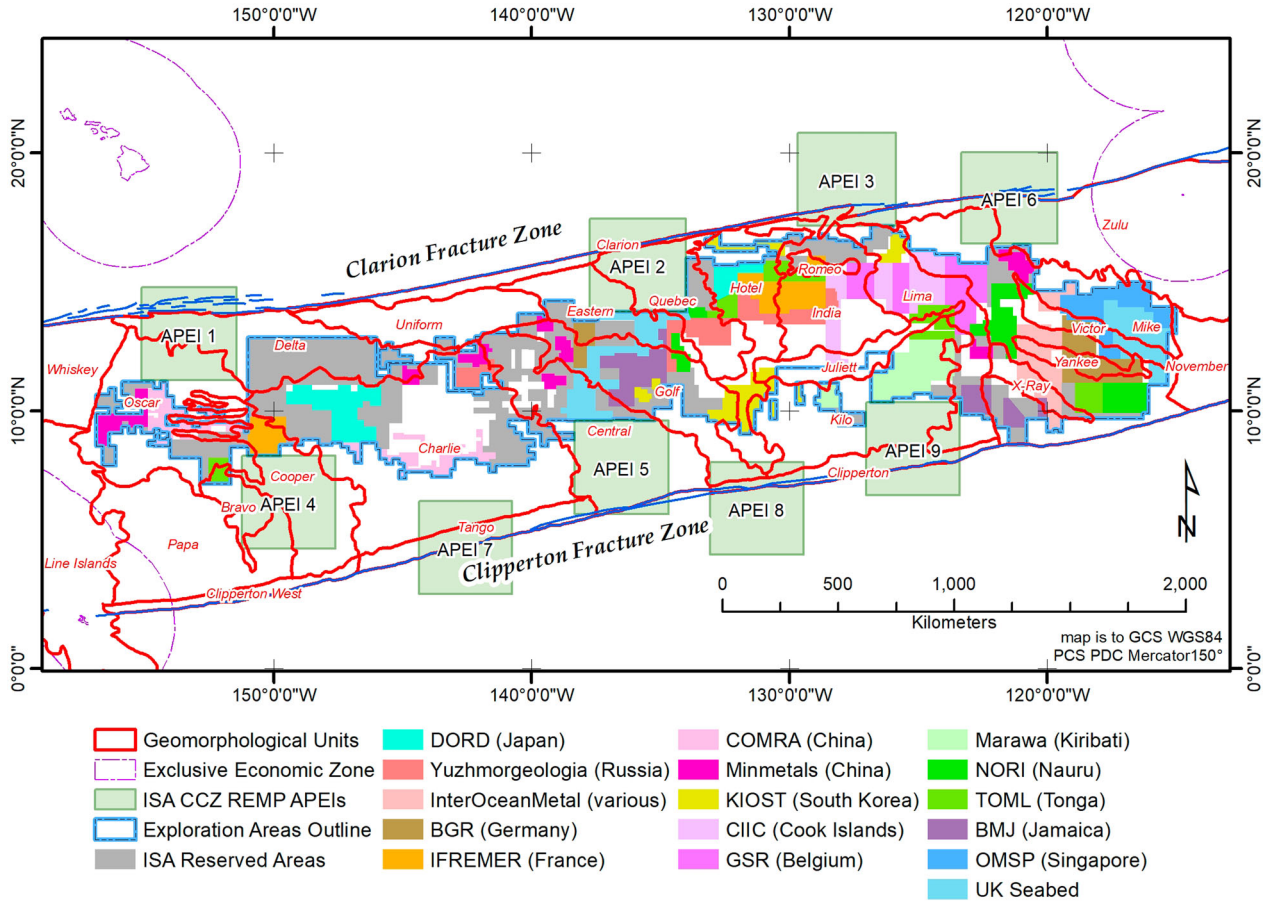


**Figure 2.** Simplified geomorphological units over ISA exploration and environmental areas in the CCZ. The border of the Exploration Areas polygon include areas of exploration under contracts with the ISA for exploration for polymetallic nodules and ISA reserved areas (International Seabed Authority, 2020) Green squares are Areas of Particular Environment Interest (APEIs) and part of the ISA Environmental Management Plan for the CCZ (International Seabed Authority, 2012).

- 2014 and then 2020 GEBCO grids from (British Oceanographic Data Centre, 2014) and (British Oceanographic Data Centre, 2020) respectively. Within the CCZ the GEBCO, 2020 grid is 87% an interpolated value guided by satellite-derived gravity data, 11% from provided multibeam data and 2% from soundings (that serve to constrain the satellite data);
- 12 kHz bathymetric images from public sources i.e. (Charlet et al., 2015; China Ocean Mineral Resources Research and Development Association, 2010; Deep Ocean Resources Development Co Ltd, 2014; Fouquet & Depauw, 2014; Global Sea Mineral Resources, 2018; Korea Institute of Ocean Science and Technology, 2014; Lipton et al., 2016; Lipton et al., 2019; Melnik & Lygina, 2010; Taymans, 2019) and from data provided by three CCZ exploration contractors (Tonga Offshore Mining Limited, Nauru Offshore Resources Inc and Marawa Research and Exploration limited);
- Publicly available ship-track multibeam data (National Centers for Environmental Information, 2020).
- Gazetted features from (GEBCO, 2020), and published seamounts and knolls derived from the GEBCO grids by (Kim & Wessel, 2011; Yesson et al., 2011).

Note that ship-track data is incorporated into the GEBCO grids, but the original track data-products are of higher resolution and were used in the interpretation.

The GEBCO bathymetric grids were processed into 100 m contour maps and colour gradient maps for use in imaging processing software and geographic information systems (GIS; Geosoft, ArcGIS and qGIS were all used). The 2020 grid benefits from finer resolution (15 arc seconds versus 30 for the 2014) although this finer point resolution means increased 'contour noise' with regards to ship-tracks. Also integrated is 12 kHz multibeam survey area from the Belgian sponsored ISA contractor GSR. The published 12 kHz bathymetric images were georeferenced and included into the GIS projects as needed, using grid data, contract vertices or natural features.

The contour data was analysed visually and after some experimentation with different depth intervals, a set of primary contours at 400 or 500 m depth intervals selected for their ability to elucidate discrete units

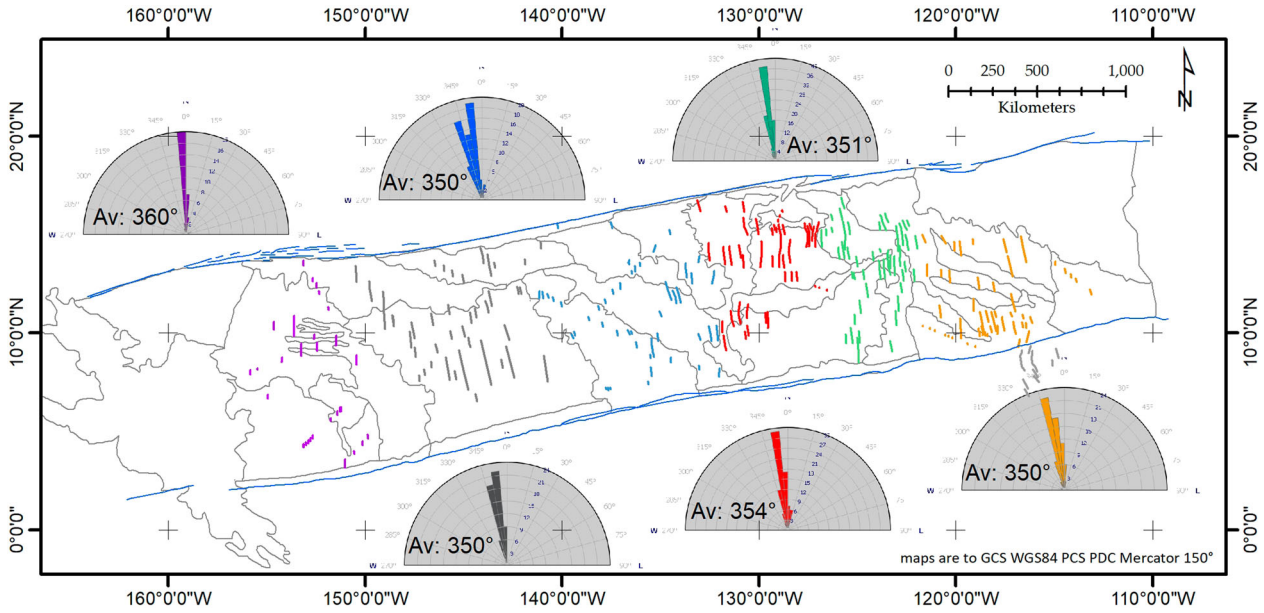


**Figure 3.** Trends of abyssal hill traces.

within the CCZ (both 2014 and 2020 GEBCO grids; Figure 4). The specific contours selected for the final interpretation are:

- 4000 m;
- 4500 m;
- 4900 m; and
- 5400 m.

The colour gradient maps helped more with picking boundaries as well as other lineaments. The gradients were also sectioned to support the interpretation further. The area of each unit was measured in GIS using a Goode homolosine projection.

CCZ wide interpretation was then made using the GEBCO grids with occasional reference to the 12 kHz images. Boundaries between features and domains as well as other structural features (lineaments and potential faults) were interpreted directly into the GIS package and the final maps thus are principally qualitative. Interpretation is generally completed at screen-scales[1] of between 1:1,000,000 and 1:2,000,000 and the final map is at 1:6,000,000. Comparison and validation of the main interpreted units was also made using hypsometric curves from the GEBCO, 2020 grid.

The interpretation of this map can be classified within the thousands of km$^2$ Tectonic Setting

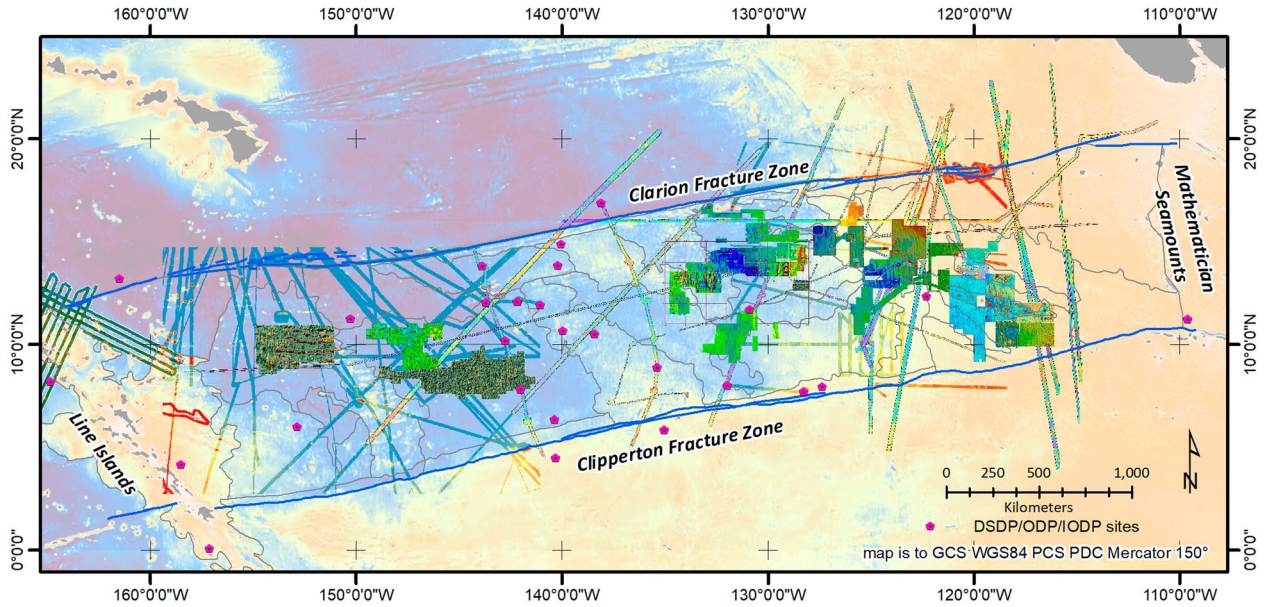


**Figure 4.** Ship-tracks and published 12 kHz images on GEBCO, 2020 grid. Note that DSDP/ODP/IODP drilling sites are included for completeness and results were not specifically used in the interpretation.

Subcomponent of the Coastal and Marine Ecological Classification Standard (CMECS (US Federal Geographic Data Committee, 2012)). This allows associated or future work, being done at a variety of scales and on a variety of themes (e.g. towed photo profile-based habitat mapping), to be integrated into the same management system.

## 3. Results

Seven types of tectonic setting geomorphological units are defined. The terms used are somewhat specific to the setting and scale of the mapped area (Figure 5), so for example differ from the terms used at the global scale by (Harris et al., 2014):

(1) Plains – i.e. of abyssal hills and valleys that comprise most of the seafloor;
(2) Transition – a plain with an overall west facing slope that in effect separates the eastern and central parts of the CCZ;
(3) Lows – diffuse to distinct areas of abyssal hills at slightly greater depths, some associated with seamount chains;
(4) Rises (Crust) – diffuse to distinct areas of variably defined abyssal hills at slightly shallower depths;
(5) Rises (Volcanic) – areas of volcanic seamounts/knolls associated with slightly elevated abyssal hills;
(6) Steps – slightly shallower blocks aligned along the main fracture zones;
(7) Trough – narrow, slightly deeper area aligned along part of one of the main fracture zones.

Each of the above units are often defined by depths relative to each other, or by the presence of a major natural feature such as a fault. This is primarily because the CCZ seafloor as a whole deepens westwards to about 128 °W (Figures 1 and 4). The boundary between, for example, a 'low' and a 'plain' in the Eastern CCZ may be some 500 m shallower than the same type of boundary in the western, older and deeper part of the CCZ. The visual interpretation used local contour intervals as a guide as well as lineaments. Knolls and seamounts are typically several hundred to thousand m shallower than their host units.

Newly defined tectonic setting geomorphological units are mostly informally named after the International Radiotelephony Spelling Alphabet, for example, Alpha, Bravo, Charlie, etc. Features with existing names are maintained (e.g. GEBCO, 2020;

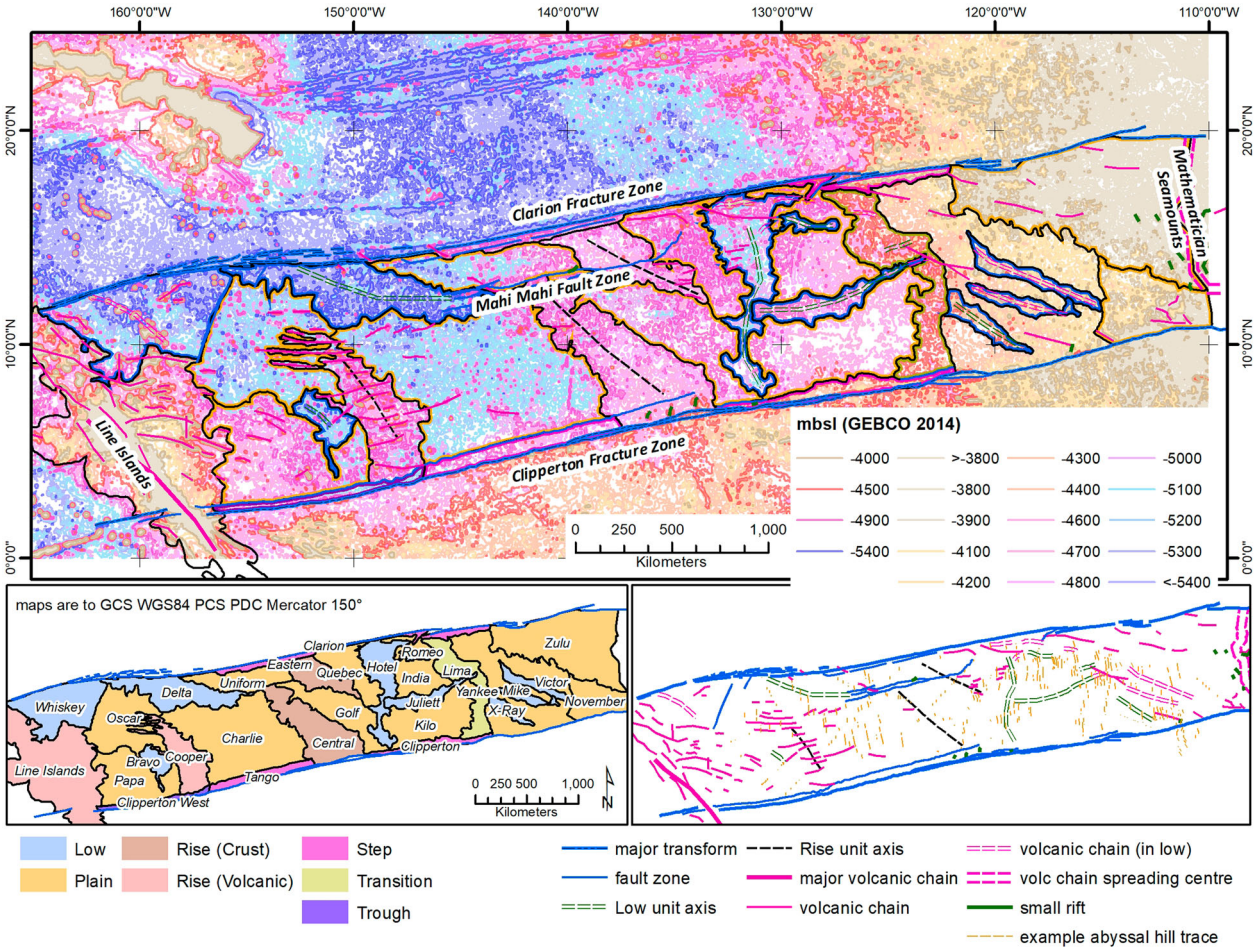


**Figure 5.** Interpreted geomorphological units and structural elements.

International Hydrographic Organization, 2008; International Seabed Authority, 2010a). As the interpretation evolved some interim units were changed or removed (i.e. merged with a neighbouring unit), thus there are some gaps in the alphabet-name sequence. Thus all names used are informal per (International Hydrographic Organization, 2008) unless indicated in the text below as being gazetted.

Most of the seabed is composed of the twelve discrete Plains and Transition, which as mentioned above deepen from the eastern end of the CCZ towards the central-western part of the CCZ, but then shallow again in the south towards the Line Islands Rise. The Transition also marks a key change from the eastern to central CCZ. The composition of these units is mostly abyssal hills but also include the above-mentioned smaller features such as volcanic cones, deeper trough grabens, and potholes.

The Plains are crosscut by Rises and Lows, which respectively comprise shallower and deeper seabed regions of abyssal hills. Both rises and lows may have knoll/seamount chains associated with them. Conditions relating to a given unit are often more complex or specific; for example, the Cooper Rise is distinctly different to the other rises, including numerous seamount chains striking at a high angle to the rise itself.

Adjacent to the main fracture zones are Steps and a Trough. These narrow blocks typically have an interpreted smaller bounding fault inside the CCZ, that reflect local vertical displacement related to the dominantly transform fracture zones. The occurrence and form of the steps and the trough are influenced by changes in the strike of the fracture zones and with the contact of rises and lows with the fracture zones.

The accuracy of the interpretation based solely on the GEBCO grid, can be tested by comparing the cases where 12 kHz MBES is also available, i.e. in terms of continuity of units over and across the edge of the 12 kHz coverage. While the interpretation process was iterative between the datasets in some areas, normally this was not needed (the GEBCO grid alone was clear enough). An example of this correlation is provided below where east–west trending ridges formed at the north-western end of the Cooper Rise (Figure 6) were interpreted from GEBCO grid. When the boundaries are overlain on higher resolution multibeam data, the correlation between the ridges and the interpreted boundaries shows good visual corroboration. Similarly, the central part of Hotel Low is clearly expressed in both data sets. This supports the proposed suitability of the GEBCO grid for interpreting seafloor features and accurately

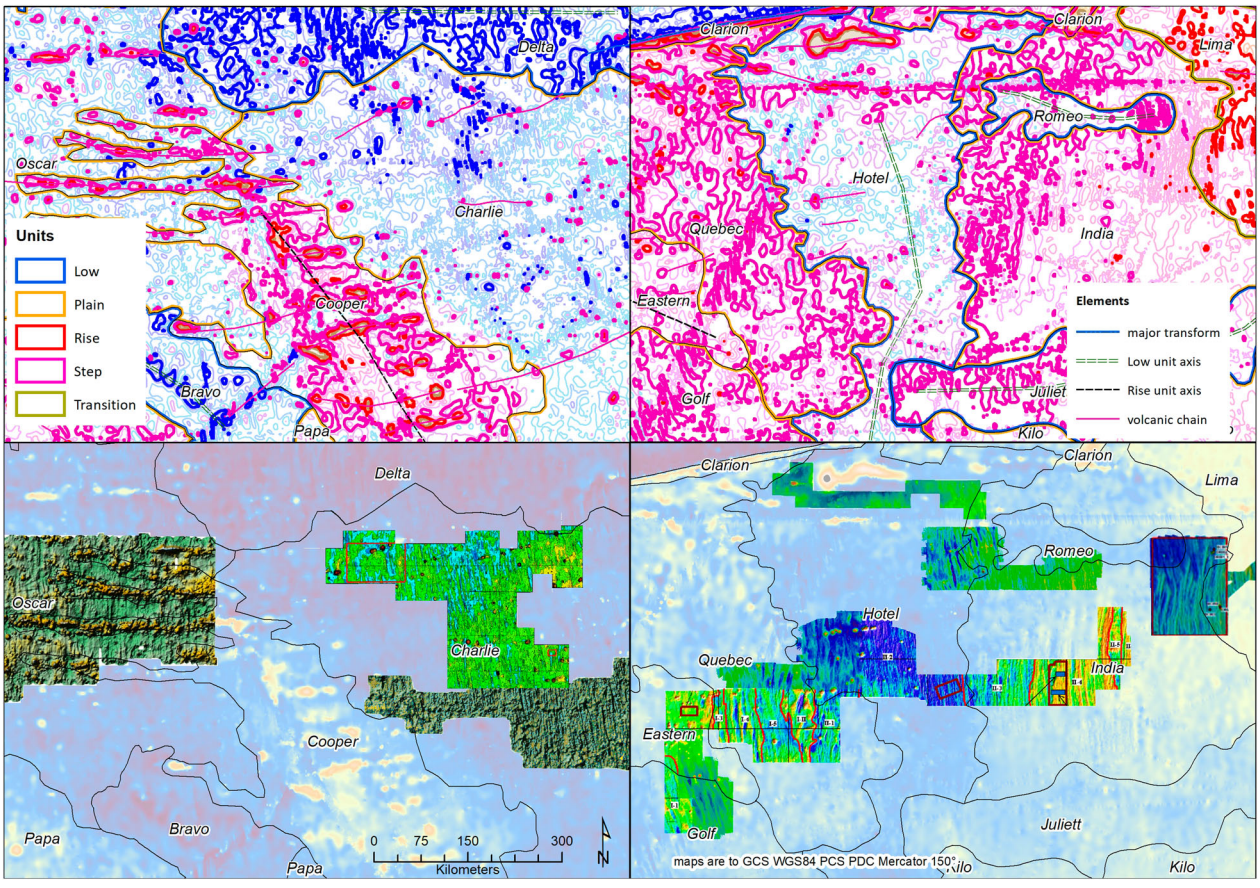


**Figure 6.** GEBCO grid versus MBES Bathymetry examples.

distinguishing between morphotectonic zones at the scales considered here.

In association with the above-mentioned interpreted tectonic setting geomorphological units, the following structural element types were also defined and interpreted (Figure 5):

(1) Major transform fractures – the Clarion and Clipperton Fracture Zones that bound the plate segment;
(2) Fault zones – smaller clear breaks in the seafloor fabric the most significant being the Mahi Mahi Fault zone;
(3) Axes of the above defined geomorphological Lows;
(4) Axes of the above defined geomorphological Rises;
(5) Major volcanic chains – includes numerous seamounts (>1000 m above the adjacent seafloor) as well as single and composite knolls. Some associated with the Lows;
(6) Volcanic chains – single and composite knolls, and occasional seamounts. Some associated with the Lows and others with the former spreading centre at the Mathematician Seamounts, and;
(7) Small rift – high angle tear-apart like structures. So far all found near the Clipperton Fracture Zone or subparallel to the Mathematician Seamounts.

Example abyssal hill strikes were also highlighted where possible (i.e. where there was 12 kHz bathymetry or clear ship-track bathymetric data), and this shows a change in abyssal hill strike between the western and central-eastern CCZ (Figure 3).

## 4. Conclusions

The CCZ is mapped at a regional scale of 1:6,000,000, based on GEBCO grids, and supported by deep sea drilling programme data, magnetic isochron interpretation and some published 12 kHz MBES coverage. The mapped geomorphological and structural units characterize each part of the CCZ, in terms of age, geomorphology, stratigraphy and structure. This includes definition of geomorphic plains, rises, lows of abyssal hills, and steps and a trough along parts of the bounding fracture zone, as well as seamount chains and internal fault zones and rifts. This interpretation should be of interest to the ISA exploration contractors who work there, as well as their regulators and sponsors.

## Software

For the map: GEBCO grids were clipped and contoured in (gdal_contour) in qGIS 3.10.7. Testing via hypsometric curves was done using native installed process in qGIS 3.10.7 and via bathymetric position in index using SAGA GIS Hill climbing clustering algorithm (courtesy Alex Fejer of Fathom Pacific). Interpretation and map compilation was done in ArcGIS 10.4.1. Terrain profiles for the cross-sections were derived using (Profile Tool 4.1.8) in qGIS 3.10.7, and assembled/interpreted in Inkscape 0.92.3. Map was compiled and set in ArcGIS 10.4.1.

For the figures: Rose diagrams were prepared using GeoRose 0.5.1. Figures were drafted either in ArcGIS 10.4.1, qGIS 3.10.7 or Inkscape 0.92.3.

## Note

1. All of the digitizing for this map used a 24" 1980 × 1080p display at 1:1,000,000 scale 10 km on the map was about 0.9 cm on the screen.

## Acknowledgments

This research was mostly completed by one of the authors (Parianos) while under the employment of Nautilus Minerals Pacific Pty Ltd, and their allocation of time to spend on the subject is gratefully acknowledged.

## Disclosure statement

No potential conflict of interest was reported by the author(s).

## Funding

This work was supported by the Portuguese Science and Technology Foundation (FCT) project UIDB/04683/2020 - ICT (Institute of Earth Sciences).

## Data availability statement

GIS data can be provided on written request to the authors.

## References

Bender, M. L., Ku, T.-L., & Broecker, W. S. (1966). Manganese nodules: Their evolution. *Science*, *151* (3708), 325–328. https://www.jstor.org/stable/1717209 https://doi.org/10.1126/science.151.3708.325

Boschman, L. M., & van Hinsbergen, D. J. J. (2016). On the enigmatic birth of the pacific plate within the Panthalassa Ocean. *Science Advances*, *2*(7), e1600022. https://doi.org/10.1126/sciadv.1600022

British Oceanographic Data Centre. (2014). *GEBCO Gridded Bathymetric Data*. Retrieved July 1, 2018, from http://www.gebco.net/data_and_products/gridded_bathymetry_data/

British Oceanographic Data Centre. (2020). *GEBCO Gridded Bathymetric Data*. Retrieved July 23, 2018, from http://www.gebco.net/data_and_products/gridded_bathymetry_data/

Broecker, W. S. (2003). The Oceanic CaCO3 cycle. In H. D. Holland & K. K. Turekian (Eds.), *Treatise on geochemistry* (1st ed., pp. 529–549). Elsevier.

Callender, E., & Bowser, C. J. (1980). Manganese and copper geochemistry of interstitial fluids from manganese nodule-rich pelagic sediments of the northeastern equatorial Pacific Ocean. *American Journal of Science*, *280*(10), 1063–1096. https://doi.org/10.2475/ajs.280.10.1063

Charlet, F., Pape, E., Juan, C., Eloot, N., Hofert, M., Halleux, L., Vanreusel, A., Van Rooij, D., & Van Nijen, K. . (2015). A multidisciplinary approach to locate polymetallic nodules and understand deep-sea environments in the GSR concession. *MIDAS Newsletter 5*. https://www.researchgate.net/publication/332029109_A_multidisciplinary_approach_to_locate_polymetallic_nodules_and_understand_deep-sea_environments_in_the_GSR_concession

Chen, C. T. A., Feely, R. A., & Gendron, J. F. (1988). Lysocline, calcuim carbonate compensation depth and calcareous sediments In the North Pacific Ocean. *Pacific Science*, *42*(3–4), 237–252.

China Ocean Mineral Resources Research and Development Association. (2010). Environmental work. In International Workshop For The Establishment Of A Regional Environmental Management Plan For The Clarion-Clipperton Zone In The Central Pacific. Kingston, Jamaica: International Seabed Authority. https://www.isa.org.jm/files/documents/EN/Workshops/2010/Pres/COMRA.pdf

Deep Ocean Resources Development Co Ltd (2014). Polymetallic nodule resources evaluation - how we are doing. in *Workshop on Polymetallic Nodule Resources Classification*. Kingston, Jamaica: International Seabed Authority. https://www.isa.org.jm/files/documents/EN/Workshops/2014a/DORD-Rev1.pdf

Fouquet, Y., Depauw, G., and GEMONOD (2014). Polymetallic nodules resource classification. In *Workshop on Polymetallic Nodule Resources Classification*. Kingston, Jamaica: International Seabed Authority. Available at: https://www.isa.org.jm/files/documents/EN/Workshops/2014a/Ifremer.pdf

GEBCO. (2020). *Undersea Feature Names Gazetteer*. Retrieved August 15, 2020, from https://www.ngdc.noaa.gov/gazetteer/

Global Sea Mineral Resources. (2018). *Environmental impact statement*. Zwijndrecht, Belgium: DEME Group. https://www2.deme-group.com/sites/default/files/isa_eia_2018_gsrnod2019.pdf

Harris, P. T., MacMillan-Lawler, M., Rupp, J., Baker, E., (2014). Geomorphology of the oceans. *Marine Geology*, *352*, 4–24. https://doi.org/10.1016/j.margeo.2014.01.011

International Hydrographic Organization. (2008). *Standardization of undersea feature names: Guidelines proposal form terminology* (4th ed.). International Hydrographic Organization and Intergovernmental Oceanographic Commission.

International Seabed Authority. (2010a). *A geological model of polymetallic nodule deposits In the Clarion-Clipperton Fracture Zone*. International Seabed Authority.

International Seabed Authority. (2010b). *A prospector's guide for polymetallic nodule deposits in the Clarion-Clipperton Fracture Zone*. International Seabed Authority.

International Seabed Authority. (2012). Decision of the Council relating to an environmental management plan for the Clarion-Clipperton Zone - ISBA/18/C/22. In International Seabed Authority (ed.)., (p. 5). International Seabed Authority. https://isa.org.jm/files/files/documents/isba-18c-22_0.pdf

International Seabed Authority. (2020). *International Seabed Authority*. Retrieved July 19, 2020, from www.isa.org.jm

Kazmin, Y. (2003). Relationships between nodule grade and abundance, and tectonics and volcanic activity in the Clarion-Clipperton Zone. In Office of Resources and Environmental Monitoring (Ed.) *Establishment of a geological model of polymetallic nodule deposits In the Clarion-Clipperton Fracture Zone of the equatorial north Pacific Ocean* (pp. 145–160). International Seabed Authority.

Kim, S.-S., & Wessel, P. (2011). New global seamount census from altimetry-derived gravity data. *Geophysical Journal International*, *186*(2), 615–631. https://doi.org/10.1111/j.1365-246X.2011.05076.x

Korea Institute of Ocean Science and Technology. (2014). Status of Korea activities in resource assessment and mining technologies. In *Workshop on Polymetallic Nodule Resources Classification*. Kingston, Jamaica: International Seabed Authority. https://www.isa.org.jm/files/documents/EN/Workshops/2014a/KIOST.pdf

Kotlinski, R., Yubko, V., & Stoyanova, V. (2009). Effects of the structural-tectonic and volcanic processes on formation of polymetallic nodules In the CCZ. In International Seabed Authority (Ed.) *Geological model workshop. International seabed authority*. https://www.isa.org.jm/files/documents/EN/Workshops/2009/VStoyanova.pdf

Lipton, I., Nimmo, M., & Parianos, J. (2016). *TOML Clarion Clipperton Zone project, Pacific Ocean*. AMC Consultants Pty Ltd. www.sedar.com

Lipton, I., Nimmo, M., & Stevenson, I. (2019). *NORI area D Clarion Clipperton Zone mineral resource estimate*. AMC Consultants Pty Ltd. www.sedar.com

Macdonald, K. C., Fox, P. J., Alexander, R. T., Pockalny, R., & Gente, P. (1996). Volcanic growth faults and the origin of Pacific abyssal hills. *Nature*, *380*(6570), 125–129. https://doi.org/10.1038/380125a0

Manea, V. C., Manea, M., & Ferrari, L. (2013). A geodynamical perspective on the subduction of Cocos and Rivera plates beneath Mexico and Central America. *Tectonophysics*, *609*, 56–81. https://doi.org/10.1016/j.tecto.2012.12.039

Matthews, K. J., Müller, R. D., Wessel, P., & Whittaker, J. M. (2011). The tectonic fabric of the ocean basins. *Journal of Geophysical Research*, *116*(B12), B12109. https://doi.org/10.1029/2011JB008413

Mayer, L. (1981). Erosional troughs In deep-sea carbonates and their relationship to basement structure. *Marine Geology*, *39*(1–2), 59–80. https://doi.org/10.1016/0025-3227(81)90028-1

McKelvey, V. E., Wright, N., & Bowen, R. (1983). Analysis of the world distribution of metal-rich subsea manganese nodules. *US Geological Survey Circular*, *886*, 1–60.

McQuaid, K., Washburn, T., & Howell, K. (2019). Annex K: Habitat mapping and environmental data – assessing representativity of the CCZ APEI network using habitat modelling and classification approaches. in *Workshop Report Deep CCZ Biodiversity Synthesis Workshop Friday Harbor, Washington, USA, 1-4 October* 2019. Kingston, Jamaica: International Seabed Authority, pp. 192–206. https://www.isa.org.jm/files/files/documents/Deep CCZ Biodiversity Synthesis Workshop Report - Final-for posting-clean-1.pdf

Melnik, V., & Lygina, T. (2010). Environmental research carried out by Yuzhmorgeologyia. In https://www.isa.org.jm/files/documents/EN/Workshops/2010/Pres/

YUZHMORGEOLOGIYA.pdf. Kingston, Jamaica: International Seabed Authority. https://www.isa.org.jm/files/documents/EN/Workshops/2010/Pres/YUZHMORGEOLOGIYA.pdf

Menard, H. W., & Shipek, C. J. (1958). Surface concentrations of manganese nodules. *Nature*, *182*(4643), 1156–1158. https://doi.org/10.1038/1821156b0

Moore, T. C., Mitchell, N. C., Lyle, M., Backman, J., & Pälike, H. (2007). Hydrothermal pits in the biogenic sediments of the equatorial Pacific Ocean. *Geochemistry, Geophysics, Geosystems*, *8*(3), n/a–n/a. https://doi.org/10.1029/2006GC001501

Morgan, C. L. (2003). Proposed model data inputs. In Office of Resources and Environmental Monitoring (Ed.) *Geological model of polymetallic nodule deposits in the Clarion-Clipperton Fracture Zone of the equatorial north Pacific Ocean* (pp. 80–95). International Seabed Authority.

Müller, R. D., Seton, M., Zahirovic, S., Williams, S. E., Matthews, K. J., Wright, N. M., Shephard, G. E., Maloney, K. T., Barnett-Moore, N., Hosseinpour, M., Bower, D. J., & Cannon, J. (2016). Ocean basin evolution and global-scale plate reorganization events since pangea breakup. *Annual Review of Earth and Planetary Sciences*, *44*(1), 107–138. https://doi.org/10.1146/annurev-earth-060115-012211

National Centers for Environmental Information. (2020). *Bathymetric data viewer*. Retrieved July 30, 2020, from https://maps.ngdc.noaa.gov/viewers/bathymetry/

Neizvestnov, Y. V., Kondratenko, A. V., & Kozlov, S. A. (2004) *Engineering geology of the Clarion-Clipperton Ore province In the Pacific Ocean*. Edited by Y. V. Neizvestnov and I. F. Glumov. Nauka.

Pälike, H. Nishi H., Lyle M., Raffi I., Klaus A., Gamage K. (2009). Integrated ocean drilling program expedition 320 preliminary report. *Pacific Equatorial Age Transect*. https://doi.org/10.2204/iodp.pr.320.2009.

Taymans, C. (2019). Benefits of the sponsoring state – Belgium. In *Presentation P-SIDs regional training & capacity building workshop*. https://www.isa.org.jm/files/files/documents/7-taymans_c.pdf

US Federal Geographic Data Committee. (2012). *Coastal and marine ecological classification standard*. http://www.fgdc.gov/standards/projects/cmecs-folder/CMECS_Version_06-2012_FINAL.pdf

van Andel, T. H., Heath, G. R., & Moore, T. C. (1975). Cenozoic history and paleoceanography of the central equatorial Pacific Ocean: A regional synthesis of deep sea drilling project data. *Geological Society of America*, *143*, 1–223. https://doi.org/10.1130/MEM143-p1

Wessel, P., Matthews, K. J., Müller, R. D., Mazzoni, A., Whittaker, J. M., Myhill, R., & Chandler, M. T. (2015). Semiautomatic fracture zone tracking. *Geochemistry, Geophysics, Geosystems*, *16*(7), 2462–2472. https://doi.org/10.1002/2015GC005853

Yesson, C., Clark, M. R., Taylor, M. L., & Rogers, A. D. (2011). The global distribution of seamounts based on 30 arc seconds bathymetry data. *Deep Sea Research Part I: Oceanographic Research Papers*, *58*(4), 442–453. https://doi.org/10.1016/j.dsr.2011.02.004